NIPPON STEEL TECHNICAL REPORT No. 58 JULY 1993

UDC669.14.018.44

Development and BOF Manufacture of Modified 9Cr-1Mo Steel Plates with Excellent Strength and Toughness

Yutaka Tsuchida*1 Kazushige Tokuno*1
Katsukuni Hashimoto*2

Abstract:

Modified 9Cr-1Mo steel plates (ASTM A 387 Grade 91) have elevated-temperature strength superior to that of Cr-Mo steels, such as ASTM A 387 Grade 11 and Grade 22, and are promising structural materials for the steam generator of fast breeder reactor (FBR). For the purpose of producing a modified 9Cr-1Mo steel plate combining excellent elevated-temperature strength and toughness with good weldability for the said application, study was made to clarify the effects of chemical composition and other parameters on the results of manufacture. As a result, the chemical composition was optimized, and with this chemistry 25, 50 and 270 mm thick plates were manufactured by an integrated process consisting of BOF steelmaking, ladle refining, and unidirectional solidification ingotmaking and rolling. It was confirmed that these steel plates have uniform chemical composition and mechanical properties through the thickness, excellent tensile strength and creep rupture strength, and good low-temperature toughness and weldability. Welded joints made of these steel plates by the GTAW, SMAW, and SAW processes also exhibit excellent mechanical properties. The Modified 9Cr-1Mo steel plate is expected to find wide use not only for FBR steam generators, but also for thermal power generation boilers and chemical reactor vessels.

1. Introduction

Chromium-molybdenum steel plates, such as ASTM A 387 Grade 11 and Grade 22, have long been used for chemical reactor vessels in oil refining and related industries. Recent improvement in reaction efficiency and the appearance of new processes, however, call for steel plates of still higher strength up to higher temperatures.

Heat transfer tubes in thermal power boiler application are used at temperatures higher than with chemical reactor vessels, for which various steels containing 9 to 12% chromium have been developed[1-3]. Among these steels is the Modified 9Cr-1Mo steel[4]

*1 Technical Development Bureau
*2 Nippon Steel Technoresearch Corporation

developed by the Oak Ridge National Laboratory (ORNL) of the United States. This steel has high-temperature strength equivalent to that of austenitic stainless steel at temperatures up to 600°C and is standardized as ASTM A 387 Grade 91, for example. Ferritic steels are high in thermal conductivity and low in the coefficient of thermal expansion, so that they are favorable in applications where thermal stress is a problem as is the case with the fast breeder reactor (FBR).

The authors developed 25 to 50 mm thick Modified 9Cr-1Mo steel plates for the shell of the FBR steam generator and 270-mm thick Modified 9Cr-1Mo steel plates as substitutes for the tube sheet forgings of the FBR steam generator. Modified 9Cr-1Mo steel plates with excellent tensile strength and creep rupture strength as well as good low-temperature toughness and weldability are successfully produced by optimizing the chemical composition within the chemical requirements of ASTM A 387 Grade 91 and establishing appropriate manufacturing conditions.

The newly developed steel is expected to find wide use in chemical reactor vessels and boilers as well as FBR steam generators. The basics of alloy composition optimization and the properties of plates manufactured by the basic oxygen furnace (BOF) process are discussed below.

2. Basic Findings

2.1 Effects of carbon, silicon, and nitrogen

The following tests were conducted while changing the steel's carbon, silicon, and nitrogen contents over the ranges of 0.02 to 0.08%, 0.09 to 0.28%, and 0.01 to 0.05%, respectively, with base values taken from the corresponding median values in the specifications of ASTM A 387 Grade 91, as shown in **Table 1**: Tensile, creep rupture, Charpy impact, and y-groove weld cracking tests[5].

As shown in **Fig. 1**, carbon does not significantly increase creep rupture strength, whereas nitrogen does in a great degree. As the nitrogen content increases, the creep rupture strength increases and, moreover, the drop of the creep rupture time decreases at the high end of the time range, as shown in **Fig. 2**. Nitrogen is thus more effective than carbon in improving the creep rupture strength.

To have a clear understanding of the effect of nitrogen on the creep rupture strength, precipitates in high-nitrogen (600 ppm N) steel and low-nitrogen (300 ppm N) steel were examined[6-7]. As shown in **Photo 1**, vanadium carbonitride precipitates with niobium carbonitride as the nucleus in a complex form like a

Table 1 Standard chemical composition for basic research

C	Si	Mn	Cr	Mo	V	Nb	N
0.08	0.30	0.45	9.0	1.0	0.2	0.08	0.05

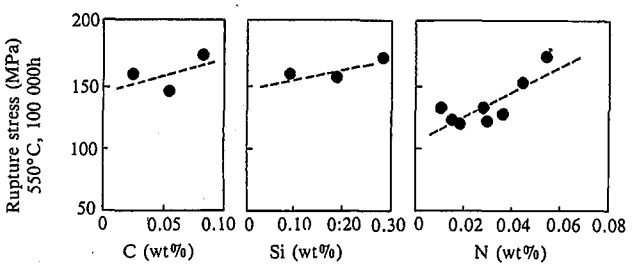

Fig. 1 Effects of carbon, silicon, and nitrogen on creep rupture strength

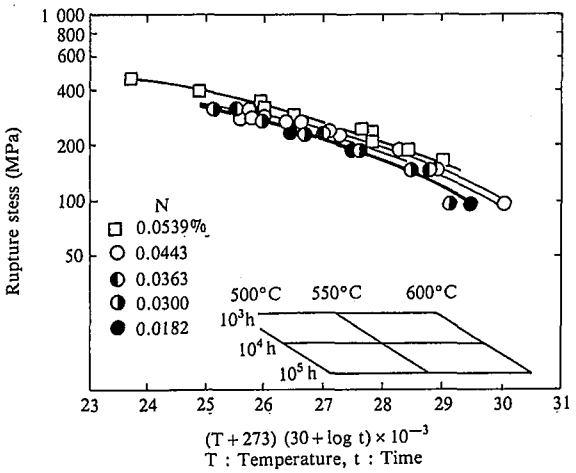

Fig. 2 Comparison of creep rupture master curves of steels with different nitrogen contents

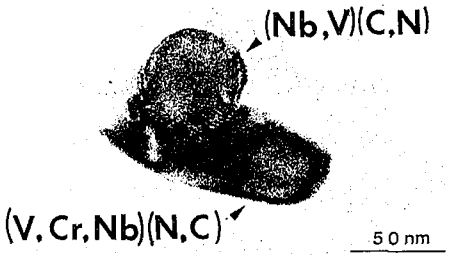

Photo 1 V-wing in 600 ppm N steel

spread wing (hereinafter called the V-wing). The spread, i.e. the length, of the V-wing increases with increasing nitrogen content as evident from the comparison of the two steels in **Photo 2**. The V-wing is thermally stable, and its length does not change even under long-time aging, as shown in **Fig. 3**[8].

One possible effect of precipitates on the creep rupture strength is the rise in the threshold stress. When the Orowan mechanism,

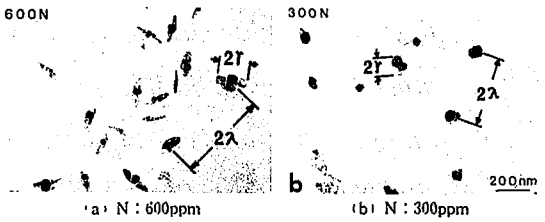

Photo 2 Comparison of V-wing size after 760°C tempering

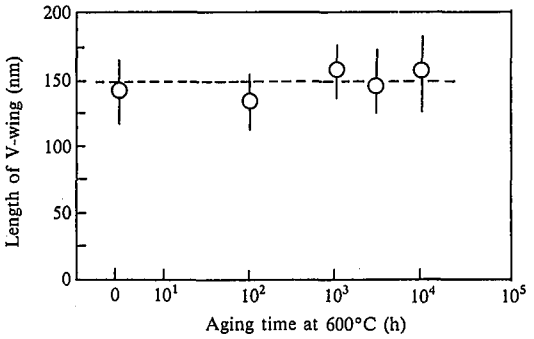

Fig. 3 Stability of V-wing length (2λ) during aging

climb mechanism, or attractive interaction of dislocation[9] is the possible strengthening mechanism, the threshold stress is given by the following approximate equation[10-12]:

$$\tau th = K \cdot Gb/(2\lambda - 2r) \quad \ldots\ldots(1)$$

where τth is the threshold stress; K is a coefficient dependent on a particular strengthening mechanism; G is the modulus of rigidity; and b is the Burgers vector. If 2λ or the dispersed condition of niobium-containing precipitates is constant in Eq. (1), the threshold stress increases with increasing V-wing size (2r). When the climb or attractive intersection of dislocation is considered, not only 2λ but the complicated form of the V-wing become a factor that cannot be ignored in the improvement of creep rupture strength.

The Charpy impact toughness falls as the carbon content falls below 0.05%, as shown in **Fig. 4**. This is due to the appearance of delta ferrite (δ-ferrite), for which there exists a lower limit to the carbon content in this respect.

The preheating temperature required to prevent weld cracking specified in the JIS Z 3158 y-groove cracking test rises with increasing carbon and nitrogen contents, as shown in **Fig. 5**. As already described, nitrogen is more effective than carbon in improving the creep rupture strength. For this reason, the carbon content is held as low as possible to inhibit the formation of δ-ferrite and obtain the desired weldability.

The effect of silicon is not clear as far as the present investigation goes. Since silicon generally adversely affects the toughness of Cr-Mo steels[13], it should be kept as low as practicable in the specified range.

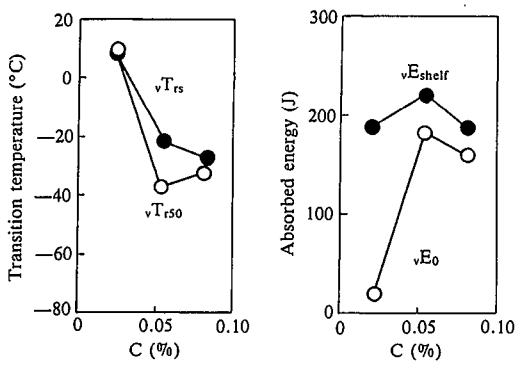

Fig. 4 Changes in Charpy impact properties with carbon content

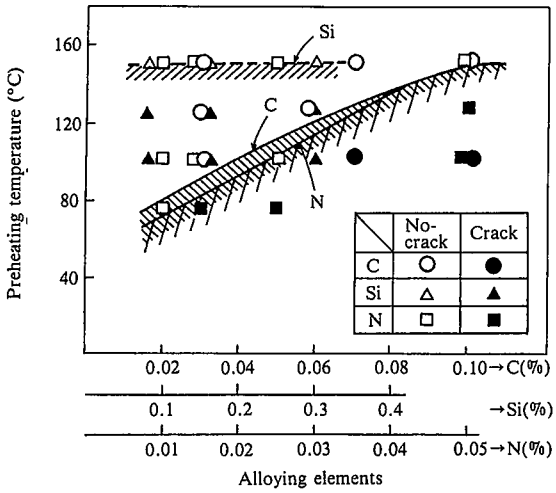

Fig. 5 Changes in critical temperature to prevent y-groove cracking with carbon, silicon, and nitrogen contents (hydrogen content determined by gas chromatography: 3.2 ml/100 g)

2.2 Vanadium content and δ-ferrite

With the base composition of 0.1%C-9%Cr-1%Mo-0.08%Nb-0.01%N, the vanadium content was changed over the range of 0.1 to 0.5%, and its effect on creep rupture strength was investigated. The creep rupture strength decreases with increasing vanadium content, as shown in **Fig. 6**. This is because the vanadium addition increases the amount of δ-ferrite, as shown in **Photo 3**. The presence of δ-ferrite not only reduces the tensile strength and creep rupture strength, but also impairs toughness, as shown in **Fig. 4**. Toughness is further impaired by the precipitation of coarse Laves phase in the δ-ferrite during service at 500 to 600°C[14].

Vanadium is basically an element that markedly improves the creep rupture strength, but it must not be added in an amount greater than that at which δ-ferrite is formed. The formation of δ-ferrite should be suppressed by lowering the addition of vanadium and other ferrite formers and by increasing the amounts of nickel, manganese, carbon, and nitrogen additions. Increasing the nitrogen content is useful also for this purpose.

2.3 Nickel content, manganese content, and retained austenite

Fig. 7 shows the changes in the room-temperature tensile strength and creep rupture strength of the 9%Cr-Mo-V-Nb steel with the addition of nickel or manganese. The nickel and manganese additions increase the tensile strength, but decrease the creep rupture time. Considering the fact that the creep rupture strength is a long-term property, this phenomenon may be explained by the increasing instability of microstructure, particularly of the carbonitride phase, with increasing nickel or manganese content.

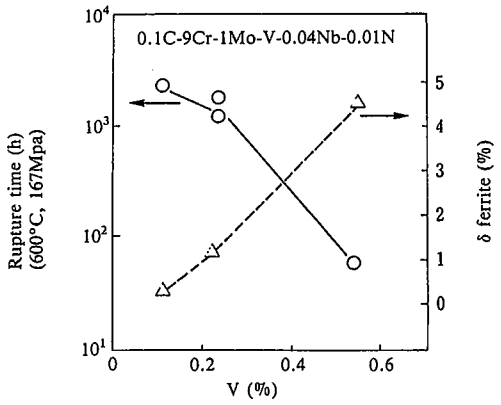

Fig. 6 Decrease of creep rupture time and increase of amount of δ-ferrite with increasing vanadium addition

Photo 3 Delta-ferrite in high-vanadium steel

The decrease in the creep rupture strength with the nickel addition is also recognized in rotor steels with 0.3 to 1% Cr, 1.25% Mo, and 0.25% V[15]. This phenomenon is attributable to the promotion of carbide precipitation and the microstructural heterogeneity which is caused by the formation of a precipitate-free zone near grain boundaries.

In high-chromium ferritic steels such as the ASTM A 387 Grade 91 steel, normalizing treatment causes the formation of retained austenite at martensite lath boundaries[16]. The amount of retained austenite can be measured by Mössbauer spectroscopy, as shown in **Fig. 8** and increases with increasing nickel or manganese. As these elements are known to sharply lower the transformation temperature, the increased amount of retained austenite may be equated with the drop of transformation temperature. Copper is presumed to have a similar effect on the retained austenite.

Retained austenite decomposes by tempering, which causes the formation of carbonitrides, while martensite precipitates carbonitrides during tempering. When the decomposing behaviors of retained austenite and martensite are compared, they naturally differ in the distribution of the carbonitride phase. This can be likened to the heterogeneous microstructure of Albrecht et al.[15] Further, retained austenite is enriched with austenite formers such as carbon and nitrogen, and these strengthening elements are reduced in the martensite lath. This probably is the reason for the decrease of creep rupture strength with the formation of retained austenite.

To improve the creep rupture strength of the ASTM A 387 Grade 91 steel, it is necessary not only to control the amount of δ-ferrite but also to reduce the amount of retained austenite by regulating the nickel, manganese and copper contents.

2.4 Effects of normalizing temperature, niobium content, and vanadium content

The normalizing temperature of the steel with the base composition of **Table 1** was changed over the range of 1,000 to 1,100°C. As shown in **Fig. 9**, it causes little change in tensile strength. The Charpy impact absorbed energy at −60°C ($_vE_{-60}$) does not change until 1,100°C, either. Along with this toughness behavior, austenite grains are prevented from coarsening.

The creep rupture strength increases with increasing normalizing temperature, as shown in **Fig. 10**. The austenite grains are kept fine as noted above, and therefore the improvement of creep rupture strength is not attributable to their coarsening. The steel has such a high alloy content that the alloying elements may not

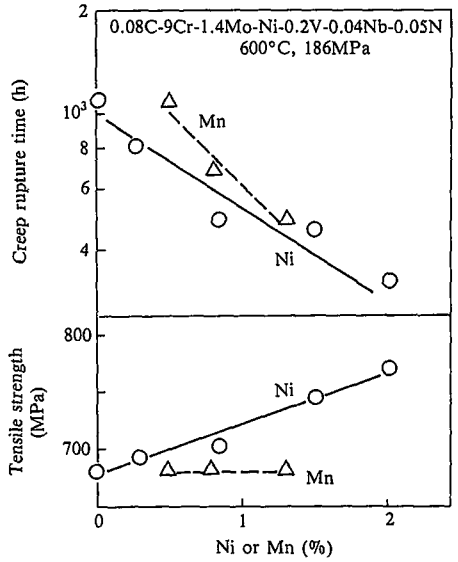

Fig. 7 Changes of creep rupture time and tensile strength by adding manganese or nickel

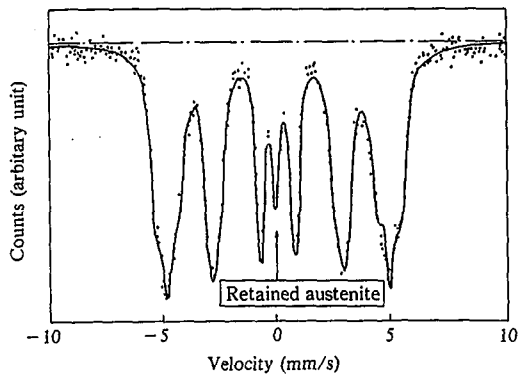

Fig. 8 Mössbauer spectrum of Modified 9Cr-1Mo steel in as-normalized condition

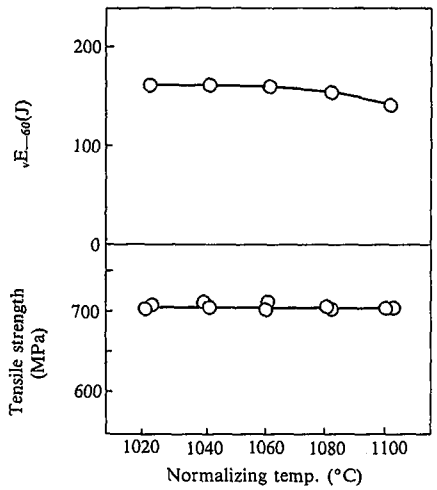

Fig. 9 Changes of tensile strength and −60°C Charpy impact absorbed energy with increasing normalizing temperature

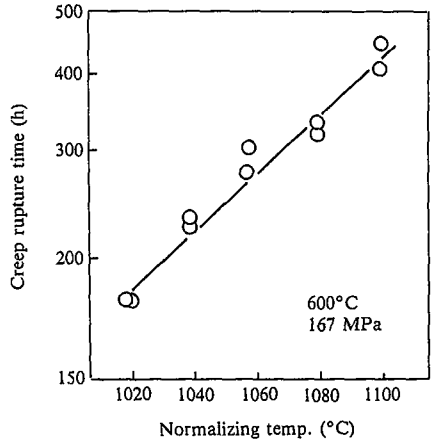

Fig. 10 Increase creep rupture time with increasing normalizing temperature

be completely brought into solid solution by heating to about 1,000°C. Therefore, the rise in the creep rupture strength may be ascribed to the increase in the amount of alloying elements going into solid solution.

Fig. 11 shows the changes in the vanadium and niobium contents of extraction residues with heating. As the chromium and molybdenum are completely dissolved at 1,000°C, they are not related to the increase of creep rupture strength with the rise of normalizing temperature to over 1,100°C. The dissolved vanadium and niobium increase with increasing heating temperature. The improvement in the creep rupture strength with the dissolution of vanadium and niobium is observed also in the 3Cr-1Mo-V-Nb steel[17]. The increase of dissolved niobium increases the amount of the niobium carbonitride that serves as nucleus for the V-wing described previously. The increase of dissolved vanadium increases the volume of V-wing precipitation or the length of the V-wing. It can be said that the dissolved niobium and vanadium combine to raise the threshold stress in Eq. (1) and improve the creep rupture strength.

The coarsening behavior of austenite grains can also be explained by niobium carbonitrides. Generally, the coarsening of austenite grains can be prevented by fine carbonitrides. As shown in **Fig. 11**, even at temperatures above 1,100°C, 0.02% or more niobium is present in the matrix. They are as fine as 0.1 μm or less in size, as shown in **Photo 4**. These fine niobium carbonitride particles act for the maintenance of fine austenite grains.

In this way, creep rupture strength and toughness, in other words austenite grain size, are significantly influenced by niobium and vanadium. It is essential to select the normalizing temperature that is high enough to secure as much niobium and vanadium as possible to go into solid solution, and is low enough to obtain a large amount of niobium carbonitrides to prevent the coarsening of austenite grains.

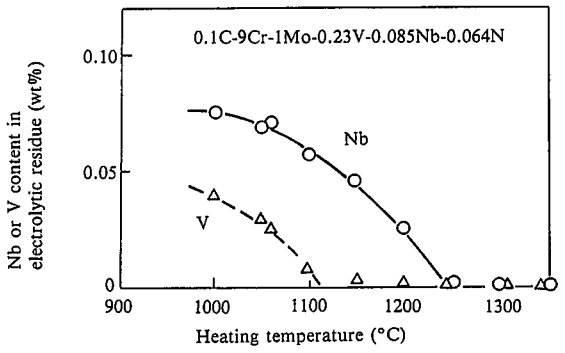

Fig. 11 Changes of vanadium and niobium contents in extracted residues with changing heating temperature

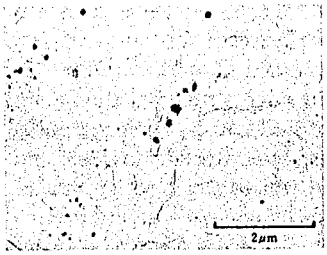

Photo 4 Niobium carbonitrides in extracted replica (normalized from 1,060°C)

2.5 Improvement of toughness by aluminum deoxidation

Electroslag remelting (ESR) was claimed to be effective in improving the toughness of the ASTM A 387 Grade 91 steel[4]. When this claim was examined, it was judged that the toughness of the steel is extremely sensitive to nonmetallic inclusions and its improvement by the ESR process is through the enhancing of cleanliness for the most part. Aluminum de-oxidation was then investigated for its benefit of enhancing cleanliness. It was found that the toughness of the steel is markedly improved by the addition of 0.005 to 0.015% aluminum, as shown in **Fig. 12**. In the actual manufacturing procedure at the mill, steel cleanliness is further improved by vacuum degassing and unidirectional solidification as well as by the aluminum deoxidation practice.

3. Mill Production Process

The BOF-based production process for the Modified 9Cr-1Mo steel plate is as schematically illustrated in **Fig. 13**. The BOF and subsequent operations such as the ladle refining process[18] limit the inclusion of such elements as nickel, copper, arsenic, tin and antimony, and assure sufficiently low phosphorus and sulfur contents, as shown in **Table 2**.

The molten steel is solidified in the unidirectional solidification ingot mold[19] illustrated in **Fig. 14**. The progress of solidification from the bottom to the top of the mold allows the sufficient flotation of nonmetallic inclusions, prevents the formation of macrosegregation like inverted-V segregation, and produces a clean and homogeneous ingot. Through-thickness composition profiles of a slab rolled from a unidirectionally solidified ingot are presented in **Fig. 15**.

The slabs are rolled, normalized and tempered into products. The 270-mm thick plates are normalized without accelerated cooling. When evaluating their mechanical properties, the plates are given a heat treatment corresponding to post-weld heat treatment at 740°C for 8.4 h.

4. Properties of Modified 9Cr-1Mo Steel Plate

4.1 Properties of 25-mm and 50-mm thick steel plates

(1) Microstructure

Photo 4 shows the microstructure of the 50-mm thick plate. The 25-mm thick plate exhibits almost the same microstructure. The microstructure is free from δ-ferrite and is composed of fine-grained tempered martensite.

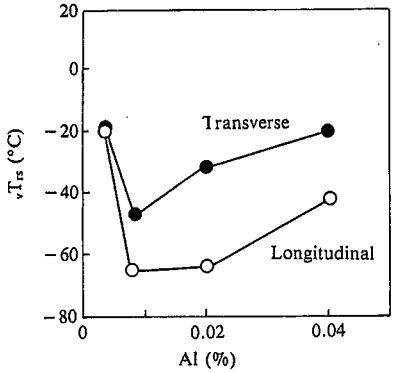

Fig. 12 Improvement in Charpy impact fracture appearance transition temperature by adding optimum aluminum

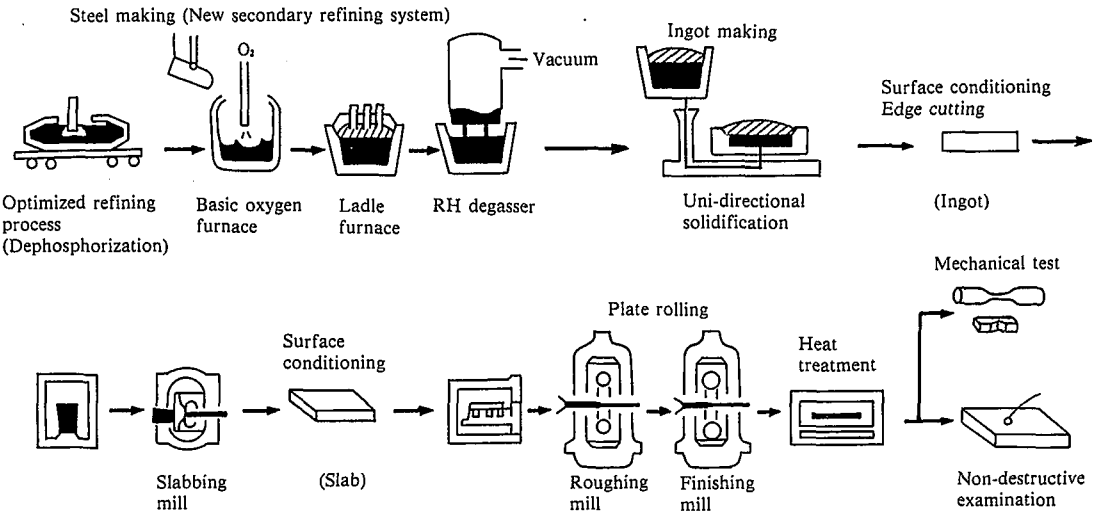

Fig. 13 Manufacturing process of Modified 9Cr-1Mo steel plate via the BOF route

Table 2 Chemical compositions of BOF steels as compared with ASTM and ASME specifications

(wt %)

	C	Si	Mn	Cr	Mo	V	Nb	Al	N	P	S	Cu	Ni	As	Sb	Sn	Plate thickness
Spec. min	0.08	0.20	0.30	8.00	0.85	0.18	0.06	—	0.030	—	—	—	—	—	—	—	—
Spec. max.	0.12	0.50	0.60	9.50	1.05	0.25	0.10	0.04	0.070	0.02	0.01	—	0.40	—	—	—	—
heat 1	0.10	0.27	0.44	8.84	0.94	0.23	0.081	0.005	0.064	0.005	0.001	0.01	0.09	0.003	0.001	0.001	25mm
heat 2	0.10	0.24	0.45	8.84	0.95	0.21	0.079	0.011	0.055	0.004	0.001	0.01	0.04	0.002	0.001	0.001	25, 50, 270mm

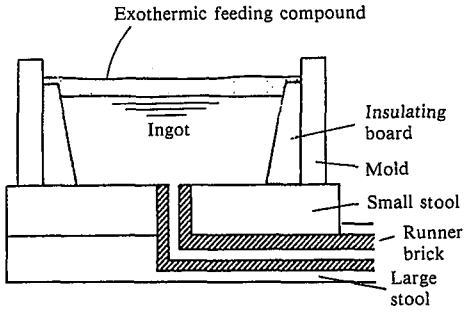

Fig. 14 Schematic illustration of unidirectional solidification ingot mold

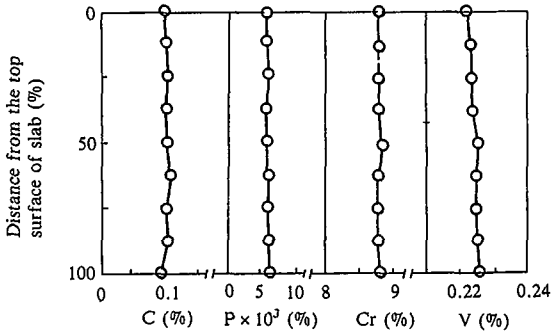

Fig. 15 Through-thickness compositional homogeneity of slab rolled from unidirectionally solidified ingot

(2) Tensile property

Fig. 16 shows the tensile property of the 50-mm thick plate in comparison with the average and minimum values of the ORNL report. The new steel retains high strength up to elevated temperatures, despite the fact that it is heated at 740°C for 8.4 h

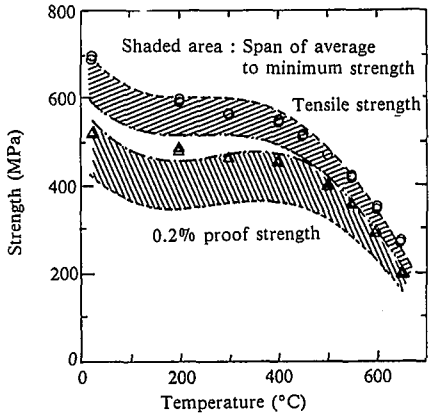

Fig. 16 Elevated-temperature tensile property of 50-mm thick plate (Transverse direction, 1/2t)

to simulate a postweld heat treatment after tempering at 760°C.

(3) Toughness

The cleanliness of the new steel is enhanced by (1) aluminum addition in the smallest necessary amount; (2) RH vacuum degassing; and (3) promotion of inclusion flotation by unidirectional solidification. The microstructure is fine-grained because of the fine dispersion of niobium carbonitrides, as shown in **Photo 5**. As a result, the steel has excellent low-temperature toughness as shown in **Fig. 17**, which is better than that of the ORNL/ESR steel[4].

This superior low-temperature toughness of the new steel hardly changes with aging as shown in **Fig. 18**, because the silicon

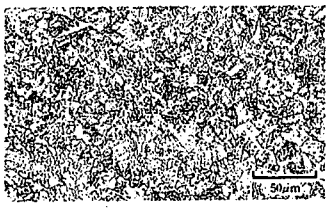

Photo 5 Microstructure of 25-mm thick Modified 9Cr-1Mo steel plate

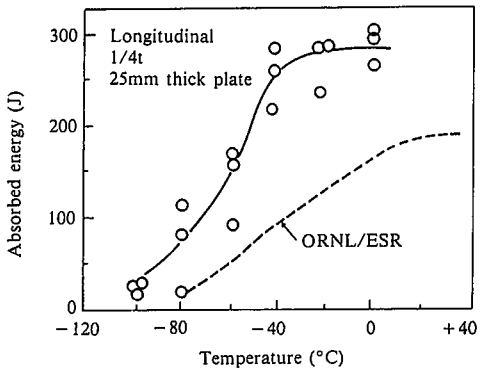

Fig. 17 Comparison of Charpy impact absorbed energy

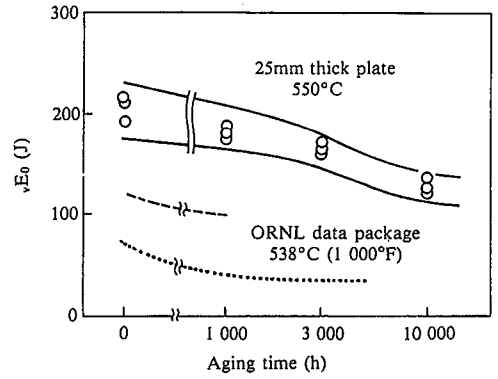

Fig. 18 Change of 0°C Charpy impact absorbed energy with aging

content is made as low as possible in the specified range[13], the contents of phosphorus and other impurity elements are also held down[20], and there is contained no δ-ferrite that promotes the formation of coarse Laves phase[14].

(4) Creep rupture property

Fig. 19 shows the creep rupture strengths of the 25-mm and 50-mm thick modified 9Cr-1Mo steel plates in comparison with the average and minimum values of the ORNL steel[4]. The minimum value is determined by obtaining the total standard deviation (SD) from the between-heat and within-heat standard deviations that are given in the ORNL data package[4] and subtracting 2.7 × SD from the average value of ORNL. The calculated minimum approximately agrees with the lower limit of the ORNL data band. The above-mentioned ORNL average values[4] are said to be overestimated and are now being reviewed.

The creep rupture strength of the new steel does not vary with plate thickness nor with in-plate position and specimen orientation. The creep rupture strength of the steel is consistently high as compared with the ORNL data[4], and the loss of creep rupture strength at the high end of the time range is small as well. This good creep rupture performance can be attributed to the optimization of the chemical composition and heat treatment. As shown in **Fig. 20**, the creep rupture elongation and reduction of area of the steel are at least 20 and 80%, respectively, which are higher than the ORNL data[4].

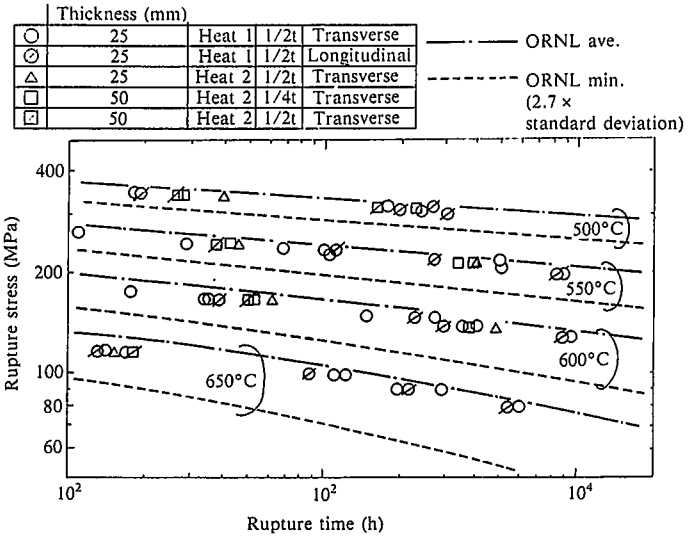

Fig. 19 Creep rupture strength of 25-mm and 50-mm thick plates

(5) Fatigue strength

Fig. 21 shows the low-cycle fatigue strength at 550°C of the new steel in comparison with the ASTM A 387 Grade 22 steel. The steel has a fatigue property comparable to that of the ASTM A 387 Grade 22 steel, although its tensile strength is higher than that of the latter steel.

4.2 Properties of 270-mm thick steel plate as a substitute for forgings

(1) Microstructure

The microstructure of the 270-mm thick plate is shown in **Photo 6**. It is composed of fine-grained tempered martensite. The steel has good hardenability, partly because of its high nitrogen

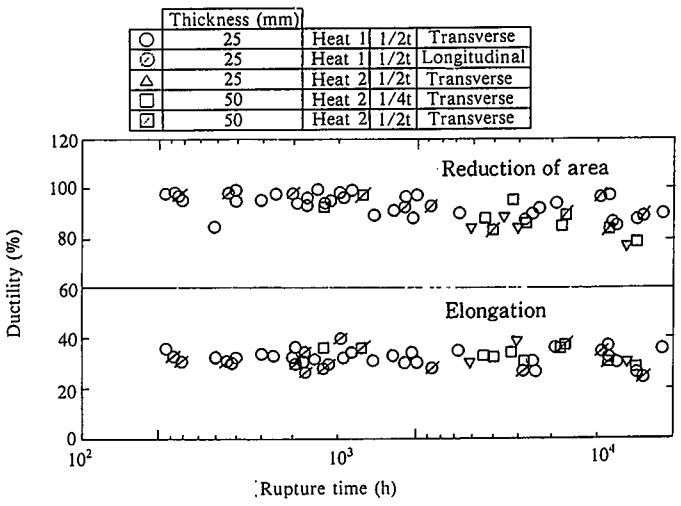

Fig. 20 Creep rupture elongation and reduction of area

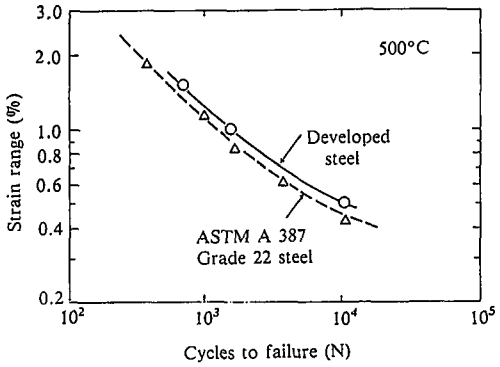

Fig. 21 Results of low-cycle fatigue test

Photo 6 Microstructure of 270-mm thick plate

content, and exhibits no proeutectic ferrite to the center of the air-cooled 270-mm thick plate.

(2) Tensile property and toughness

Fig. 22 shows the through-thickness tensile property and Charpy impact absorbed energy distributions of the 270-mm thick plate. The 0.2% offset yield strength and tensile strength are high to the center, despite the fact that the plate is air cooled for normalizing. Further, tensile ductility at fracture and Charpy impact absorbed energy are both good and uniform in the thickness direction. These properties do not appreciably change with specimen orientation.

(3) Creep rupture strength

Fig. 23 shows the creep rupture test results of the 270-mm thick steel plate at the quarter thickness in the longitudinal and short-transverse directions as compared with the ORNL data. The creep rupture strength of the steel scarcely varies according to the direction, and is always higher than the minimum value of the ORNL data. The fracture elongation and reduction of area are also good at 20 and 80%, respectively.

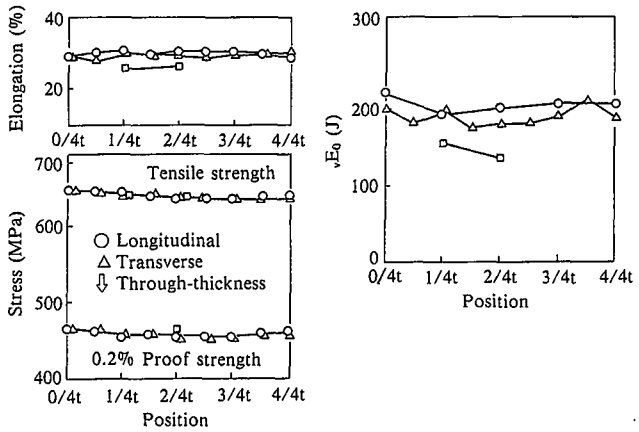

Fig. 22 Through-thickness uniformity of the properties of 270-mm thick plate

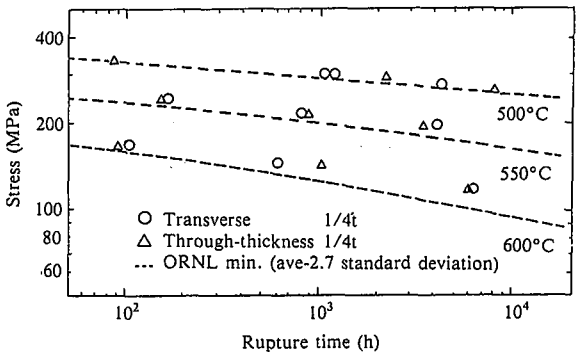

Fig. 23 Creep rupture strength of 270-mm thick plate

4.3 Weldability and welded joint properties

(1) Cold cracking resistance

The cold cracking resistance of 25-mm and 270-mm thick plates was evaluated by the y-groove cracking test. Specimens measuring 25 mm in thickness were machined from quarter-thickness and mid-thickness positions. As shown in **Fig. 24**, the maximum preheating temperature to prevent cracking is lower than 150°C and is equivalent to that of the ASTM A 387 Grade 22 steel plate.

(2) Welded joint properties

The 25-mm thick plates and 25-mm thick specimens machined from the quarter-thickness of the 270-mm thick plates were subjected to the gas tungsten arc welding (GTAW), shielded metal arc welding (SMAW) and submerged arc welding (SAW) processes, and then to post-weld heat treated at 740°C for 8.4 h, to evaluate the welded joint properties. The welding materials used are newly developed ones[21] whose chemical compositions of are summarized in **Table 3**.

The weld metal and welded joints as well as the base metal have sufficient tensile strength, which is equivalent to the average tensile strength of the ORNL data[4]. The welded joints have high enough toughness in weld metal, fusion line and heat-affected zone. They also have satisfactory resistance to cracking during bending, as shown in **Photo 7**.

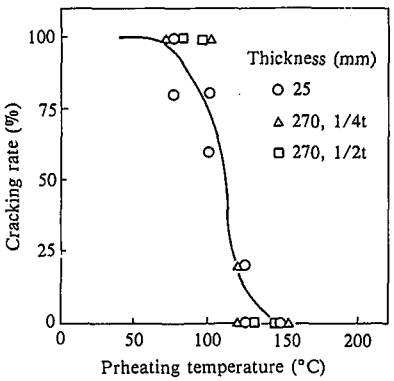

Fig. 24 Results of y-groove cracking test on 25-mm and 270-mm thick plates

Table 3 Chemical compositions of various weld metals

(wt %)

	C	Si	Mn	Cr	Mo	V	Nb	N
GTAW	0.06	0.23	0.41	9.05	0.89	0.20	0.07	0.032
SMAW	0.06	0.38	1.34	8.82	0.94	0.23	0.05	0.030
SAW	0.08	0.54	1.52	8.90	0.90	0.34	0.06	0.038

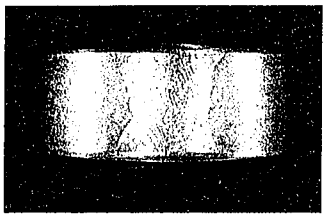

Photo 7 Appearance of welded joint after bending test

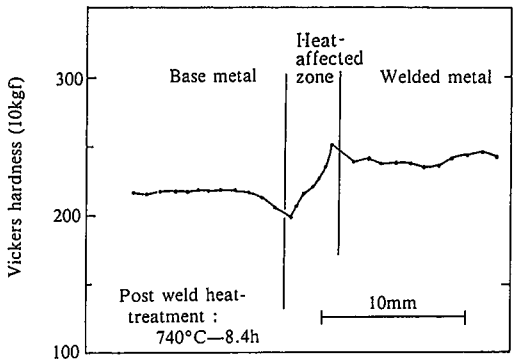

Fig. 25 Hardness traverse of submerged arc welded joint

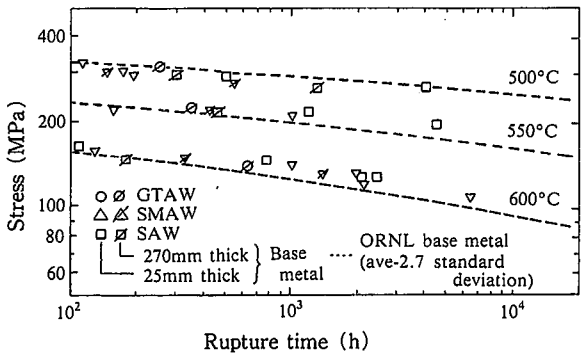

Fig. 26 Creep rupture strength of various welded joints

Fig. 25 shows the hardness traverse of a submerged arc welded joint. Although some softening is observed in the heat-affected zone (HAZ), the welded joint keeps the hardness of HV 200 or above. The creep rupture strength of the welded joint is higher than the minimum creep rupture strength[4] of the ORNL base metal, as shown in **Fig. 26**.

5. Conclusions

The Modified 9Cr-1Mo steel plate (ASTM A 387 Grade 91) has elevated-temperature strength superior to that of Cr-Mo steels, such as ASTM A 387 Grades 11 and 22, and is regarded as a promising structural material for fast breeder reactors and other high-temperature applications.

The effects of chemical composition and manufacturing conditions including heat treatment were clarified. The chemical composition and manufacturing conditions were optimized from the standpoints of creep rupture strength, low-temperature toughness, and weldability. According to the results obtained, 25-mm to 50-mm thick plates for the steam generators of fast breeder reactors (FBRs) and 270-mm thick plates for the tube sheets of FBR steam generators were produced by the processing route of BOF steelmaking, ladle refining, and unidirectional solidification ingotmaking. It was confirmed that the proposed steel plates are uniform in chemical composition and mechanical properties, excellent in tensile strength and creep rupture strength, and good in low-temperature toughness and weldability.

The Modified 9Cr-1Mo steel is being used for heat transfer tubes (ASTM A 231 Grade T91) in ultra-supercritical pressure boilers. The steel has excellent elevated-temperature strength in the base metal and welded joints, and is an ideal material for elevated-temperature reheat steam tubes in the field of thermal power boiler. Since it has a chromium content, it is believed to exhibit excellent corrosion resistance in such elevated-temperature applications as chemical reactor vessels.

References

1) Otoguro, Y. et al.: Seitetsu Kenkyu. (311), 54 (1983)
2) Yukitoshi, T. et al.: Sumitomo Metals. 27 (1), 34 (1975)
3) Kinoshita, K.: Nippon Kokan Technical Report. (62), 601 (1973)
4) Patriarca, P.: Modified 9Cr-1Mo Steel Technical Program and Data Package for Use in ASME Section I and VIII Design Analyses. ORNL, June 1982
5) Tsuchida, Y. et al.: 6th Intern. Conf. on Pressure Vessel Tech. Beijing, 1988
6) Tokuno, K. et al.: Scripta Metallurgica. 25, 871 (1991)
7) Hamada, K. et al.: Research Report of 123rd Committee, Japan Society for the Promotion of Science. Vol. 33, 1991, p. 9
8) Tokuno, K. et al.: JOM. (April), 25 (1992)
9) Gotoh, M. et al.: J. Jpn. Inst. Met. 50, 154 (1986)
10) Arzt, E., Ashby, M.F.: Scripta Metallurgica. 16, 1285 (1982)
11) Arzt, E., Wilkinson, D.S.: Acta Metallurgica. 34, 1893 (1986)
12) Srolovitz, D. et al.: Scripta Metallurgica. 16, 1401 (1982)
13) Doi, H. et al.: CAMP-ISIJ. 2, 1808 (1989)
14) Hosoi, Y. et al.: J. of Nuclear Materials. A141-A143, 461 (1986)
15) Albrecht, J. et al.: Mechanical Working and Steel Processing. 27, 163 (1989)
16) Tokuno, K., Takeda, T.: TMS Annual Meeting, Las Vegas, U.S.A.,
17) Tsuichida, Y. et al.: CAMP-ISIJ. 2, 1724 (1989)
18) Ohnishi, Y. et al.: Iron & Steelmaker. 12 (2), 29-34 (1985)
19) Saeki, T. et al.: Tetsu-to-Hagané. 71, S266 (1985)
20) Tachibana, H. et al.: Tetsu-to-Hagané. 73, S499 (1987)
21) Hirano, T. et al.: Pre-prints of the National Meeting of JWS. 41, 1987